Lower-Tropospheric Enhancement of Gravity Wave Drag in a Global Spectral Atmospheric Forecast Model

SONG-YOU HONG, JUNG CHOI, EUN-CHUL CHANG, AND HOON PARK

Department of Atmospheric Sciences, Global Environment Laboratory, Yonsei University, Seoul, South Korea

YOUNG-JOON KIM

Naval Research Laboratory, Marine Meteorology Division, Monterey, California

(Manuscript received 23 March 2007, in final form 15 October 2007)

ABSTRACT

The impacts of enhanced lower-tropospheric gravity wave drag induced by subgrid-scale orography on short- and medium-range forecasts as well as seasonal simulations are examined. This study reports on the enhanced performance of the scheme proposed by Kim and Arakawa, which has been used in the National Centers for Environmental Prediction (NCEP) Global Spectral Model since 1997. The performance is evaluated against a traditional upper-level drag scheme that is also available in the model. The experiment results reveal that the Kim–Arakawa scheme improves the movement and intensity of an extratropical cyclone and a continental high pressure system that was accompanied by heavy snowfall over Korea on 14–15 February 2001. The monthly verification for medium-range forecasts in December 2006, which are initialized by the NCEP operational analysis, demonstrates overall improvements in the forecasts of large-scale fields in the Northern Hemisphere. Moderate improvements are also found in the seasonal simulation of December–February for the years 1996/97, 1997/98, and 1999/2000. This study concludes that the enhanced lower-level drag should be properly parameterized in global atmospheric models for numerical weather prediction and seasonal prediction.

1. Introduction

At present, global numerical weather prediction models run with horizontal resolutions that cannot typically resolve atmospheric phenomena smaller than about 10–100 km. Many atmospheric processes have shorter horizontal scales than these scales and some of these "subgrid scale" processes interact with one another and affect the larger-scale atmosphere in important ways. Atmospheric gravity waves are one such unresolved process. The dissipation of these waves produces synoptic-scale body forces on the atmospheric flow, known as gravity wave drag (GWD). The momentum dissipation is adjusted vertically, while limiting the gravity wave growth when the Froude number exceeds a critical value and depositing momentum. The spatial scales of these waves (in the range of approximately 5–500 km horizontally) are too short to be fully captured by model grids, and so GWD must be parameterized (see Kim et al. 2003 and the references therein).

The first-generation GWD parameterization schemes for large-scale models with relatively low model tops were developed for mountain waves (e.g., Palmer et al. 1986). The first formulations were single-wave parameterizations based on the two-dimensional wave theory, utilizing the "saturation hypothesis" (Lindzen 1981). One of the main tasks of these schemes was to separate the stratospheric polar night jet from the tropospheric subtropical jet by reducing the overall magnitude of the jets and creating stronger easterly wind shear in the upper troposphere.

Subsequent development of GWD parameterization was motivated by findings from mountain-wave simulations and observations, as well as the need for increased lower-level drag in large-scale models. The

Corresponding author address: Song-You Hong, Dept. of Atmospheric Sciences, Yonsei University, Seoul 120-749, South Korea.
E-mail: shong@yonsei.ac.kr

DOI: 10.1175/2007WAF2007030.1

lower-level wave breaking occurring in the downstream region may induce a critical layer below which the wave energy is trapped and, if the conditions are met, enhance the drag through resonant amplification of nonhydrostatic waves (e.g., Kim and Arakawa 1995, hereafter KA). Moreover, the blocking of lower-level flow, due to subgrid-scale orography, may enhance the surface drag dramatically (e.g., Lott and Miller 1997); more discussion on flow blocking will be given later.

This study investigates the effects of GWD induced by subgrid-scale orography (hereafter GWDO) on the short- and medium-range forecasts and also seasonal simulations in the National Centers for Environmental Prediction (NCEP) Global Spectral Model (GSM). The performance of the KA scheme is evaluated against a conventional upper-level GWDO scheme. An extratropical cyclone over East Asia in February 2001 is selected to investigate the intrinsic differences in wave breaking between the two schemes, and the period of December 2006 is chosen for statistical evaluation of the medium-range forecasts. Three-year winter climatology is also chosen for evaluation of a seasonal simulation. Section 2 describes the model and experimental design, together with the implementation methodology of the KA scheme. Results are discussed in section 3, and the concluding remarks are provided in the final section.

2. The model and experiment designs

a. The National Centers for Environmental Prediction (NCEP) Global Spectral Model (GSM)

The model used in this study is a version of the NCEP GSM (Kanamitsu et al. 2002a). This model has followed a path rather separate from the ongoing development of the operational NCEP medium-range forecast models. For example, the NCEP GSM herein has multiple options for the physics package. The physics package used in this study follows the version that went into operation for medium-range forecasts as of the year 2000, except for the vertical diffusion scheme of Hong et al. (2006) and GWDO. Model physics include long- and shortwave radiation, cloud–radiation interaction, planetary boundary layer (PBL) processes, deep and shallow convection, large-scale condensation, GWDO, enhanced topography, simple hydrology, and vertical and horizontal diffusions.

b. Implementation of the KA GWDO scheme

The scheme of Alpert et al. (1988, hereafter AL) is a typical GWDO scheme based on Lindzen's wave saturation theory, which considers mainly the upper-level wave breaking. A typical effect of this parameterization is very large midlatitude lower-stratospheric drag that has a direct impact on the stratospheric jet and an indirect impact on the surface westerlies through the secondary circulation induced by the stratospheric drag.

As compared with the AL scheme representing the upper-level wave drag in terms of the standard deviation of subgrid-scale orographic heights, the KA scheme additionally includes the effects of lower-level wave breaking mainly in downstream regions with the aid of orographic asymmetry (OA) and orographic convexity (OC). The OA measures the asymmetry of subgrid-scale orography and its relative location to the model grid box. The OA has positive value over the downstream and negative value over the upstream grid box areas. The OC represents the sharpness (and slope) of the mountain(s), which is linked to the characteristics of the corresponding mountain wave.

The formulations for the GWDO parameterization that is implemented in this study are formally the same as those of KA except for the determination of the reference level. In KA the definition of the reference level was the height of the PBL, whereas in this study it is the larger value of $2\sigma_h$, following Kim and Doyle (2005), where σ_h is the standard deviation of subgrid-scale orographic heights, or the height of the PBL. Orographic statistics including the mean, variance, asymmetry, and convexity are derived from a 30-arcsecond resolution digital elevation model (DEM) dataset (Hong 1999). A detailed method of computing the orography statistics is given in KA and Kim and Doyle (2005; excluding the newly introduced orographic direction). Note here that the AL scheme does not include the orientation of the subgrid-scale orography as was done in KA through OA.

The GWDO scheme that went into operation at NCEP in 2000 includes the lower-level drag enhancement effects utilizing the KA algorithm, as documented in Alpert et al. (1996). The major difference in the implementation of the KA scheme between the Alpert et al. (1996) and this study is the determination of the reference level as described above. Preliminary results (not shown) reveal that the performance of the KA scheme is highly sensitive to the behavior of the vertical diffusion algorithm in stable boundary layer conditions. This GWDO scheme was further complemented at NCEP (Alpert 2004) by adding the blocking effects of subgrid-scale flow based on the work of Lott and Miller (1997) and went into operation in the year 2004. This scheme is used in conjunction with the GWDO scheme based on Alpert et al. (1988, 1996) and KA. The more recent version of the KA scheme (Kim and Doyle 2005)

also includes a separate optional formulation for flow blocking. The difference between the drag due to flow blocking and GWDO is discussed in Kim and Doyle (2005).

The GWDO scheme used in this study, however, does not include the flow-blocking parameterization, which has been included in several recent orographic drag parameterizations (e.g., Lott and Miller 1997; Webster et al. 2003; Alpert 2004). A detailed discussion of the flow-blocking parameterization is, therefore, beyond the scope of this study. Although we recognize the subsequent development issues of the GWDO in the NCEP operational models and the interaction issues between the GWDO and other physical processes, our study will focus on the examination of the fundamental role of enhanced lower-level wave drag in the GWDO scheme on numerical weather prediction and seasonal simulations.

c. Experimental setup

Two GWDO schemes, respectively those of AL and KA, are compared using three sets of experiments: a short-range forecast, a medium-range forecast, and a seasonal simulation. First, we investigate the fundamental role of the enhanced wave drag in the lower troposphere by selecting an extratropical cyclogenesis case that produced heavy snowfall over Korea at 2100 UTC 14 February–1800 UTC 15 February 2001. The model was integrated for 120 h, starting from 0000 UTC 13 February 2001. Initial conditions are derived from the NCEP–Department of Energy (NCEP–DOE) Reanalysis II dataset (R-2; Kanamitsu et al. 2002b). We focus on the results from a model with the horizontal resolution corresponding to the spectral truncation of T62 (triangular truncation of wavenumbers at 62, corresponding roughly to about 200 km), which are compared with the results of T126- and T214-resolution runs. Note that the T62 analysis is used as the initial conditions for the higher-resolution runs as well. The resolutions of T126 and T216 are equivalent to about 100 and 50 km, respectively. The number of vertical layers is 28 with the model top at 4 hPa. The impact of GWDO forcing on the large-scale field is investigated using the case studies.

Second, a month period is chosen for statistical evaluation of the KA scheme based on the skill of medium-range forecasts. Ten-day forecasts, with a horizontal resolution of T214, are performed every 0000 and 1200 UTC for the month of December 2006. In this experiment, initial data are obtained from the operational Global Data Assimilation System (GDAS; Parrish and Derber 1992). Note that the GDAS analysis may be influenced by the GWDO parameterization as it is present in the guess field, but the richness of observations in the Northern Hemisphere would likely minimize this problem. Statistical verification of large-scale fields is computed against the NCEP GDAS analysis.

Third, seasonal simulations are performed for boreal winters in December–February (DJF) of the years 1996/97, 1997/98, and 1999/2000. To estimate and filter out the unpredictable part of the flow, five-member ensemble runs are performed. The ensemble runs are initialized at 0000 UTC 1–5 November. Each simulation thus consists of 15 runs. Initial conditions are derived from the R-2 data. As the surface boundary condition, the observed sea surface temperature (SST) data were used with a resolution of 1° (Reynolds and Smith 1994) during the simulation period. The horizontal resolution of the model for seasonal simulation is T62 and the vertical resolution is the same as that for the medium-range forecasts. Based on the seasonal simulation, the impact of GWDO forcing on the large-scale circulation and the simulated climatology will be evaluated. A composite of 3-yr simulations is presented and discussed as the purpose of the seasonal simulation is to examine the capability of a GWDO scheme to reproduce the observed climatology.

3. Results

a. Fundamental differences between the AL and KA schemes

Figure 1a shows that the results from the AL scheme exhibit a large amount of wave stress throughout the height in the midlatitudes of the Northern Hemisphere (NH; 20°–90°N), which is mainly induced by the Tibetan Plateau and the Rockies. Wave breaking, as realized by the vertical gradient of the wave stress, appears in the upper troposphere and lower stratosphere over these areas (Fig. 1c). In the Southern Hemisphere (SH; 20°–90°S), wave breaking is seen in the mid- and upper troposphere, which is mainly caused by the Antarctic continent and the Andes. On the other hand, in the case of the KA scheme (Figs. 1b and 1d), a large amount of stress is mostly limited to the near surface, inducing a substantial amount of wave breaking in the lower troposphere. Because of the overall reduced stress, the deceleration of winds in the upper-level breaking region is relatively weak with the KA scheme. In the NH, the vertical range of the wave stress is similar to that of the AL scheme, but generally weaker in magnitude, indicating weaker deceleration of the zonal winds in the upper troposphere and lower stratosphere

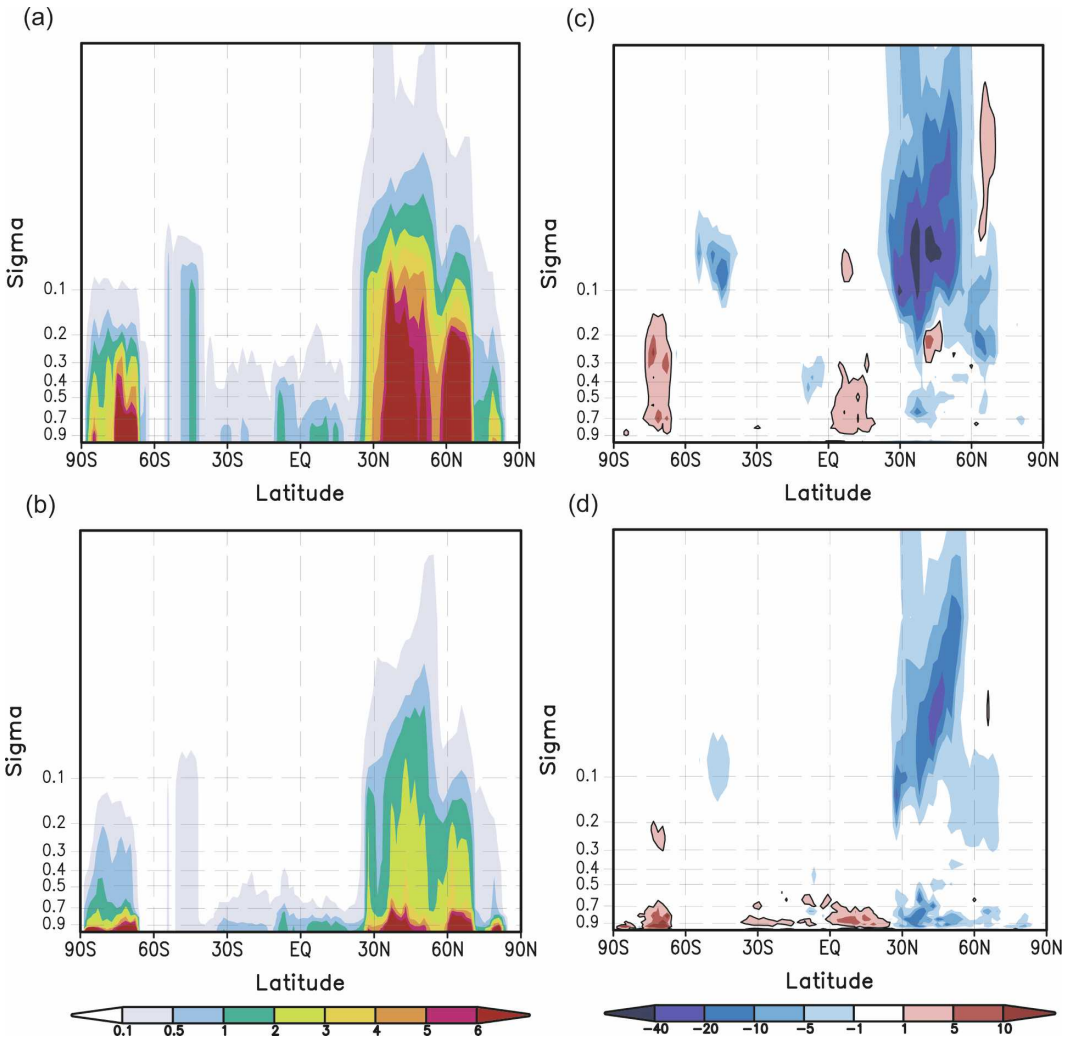

FIG. 1. Zonal mean of the gravity wave stress (10^{-2} N m^{-2}) at 0000 UTC 18 Feb 2001 (120-h forecast time), obtained from forecasts with the (a) AL and (b) KA schemes, and (c), (d) the corresponding zonal mean zonal acceleration (10^{-6} m s^{-2}).

than in the AL scheme. In the tropics, the stress is small due to relatively low orography. These characteristics of the KA algorithm in comparison with the AL scheme shown in Fig. 1 are commonly identified in the seasonal simulations. In other words, the lower-level drag enhancements and subsequent vertical stress gradient in the KA scheme (Fig. 1b), which contrast with the more constant stress shown in the AL scheme (Fig. 1a), also appear in the seasonal simulation (not shown).

In Fig. 1, it is also noted that the amount of wave stress itself in the lower troposphere is similar between the two schemes. It is thus the vertical gradient of the stress that makes the distribution very different between the two schemes: The wave breaking occurs at far lower vertical levels in the KA scheme than in the AL scheme. The AL scheme introduces significant upper-level GWDO, which can affect the low levels through the GWDO-induced secondary circulation, but its effect seems to be smaller than the direct imposition of low-level GWDO by the KA scheme.

b. *Short-range forecasts*

Table 1 presents the skill scores from 48- and 72-h forecast experiments with the AL and KA schemes for various resolutions in terms of the root-mean-square error (RMSE) and pattern correlation coefficients (PC) over East Asia. The PC as used here is calculated without removing any climatology to compare the patterns of a local system between the forecast and the observation. The results demonstrate that the inclusion of enhanced lower-level GWDO improves the distribution of the sea level pressures in terms of the RMSE

TABLE 1. Skill scores of the sea level pressure at 48 and 72 h from the forecast experiments with the AL and KA schemes for various resolutions in terms of the RMSE (hPa) and pattern correlation coefficients (PC) over 25°–50°N and 110°–145°E for the case with extratropical cyclogenesis around Korea, starting from 0000 UTC 13 Feb 2001.

	48-h forecast		72-h forecast	
Time	RMSE	PC	RMSE	PC
AL T62	2.23	0.91	4.79	0.85
AL T126	3.02	0.87	3.55	0.93
AL T214	2.63	0.89	3.11	0.95
KA T62	1.94	0.94	3.20	0.91
KA T126	2.99	0.93	2.00	0.96
KA T214	2.42	0.94	1.90	0.96

and PC. It is noted that the skill improvement is not parallel to the resolution increase. It is possible that the changes due to resolution increases may not be large and systematic, and thus not statistically significant. It is, however, hard to expect a linear response especially from experiments over a local area in a global model.

Figure 2 validates the sea level pressure patterns at 48-h forecast time. The intensity of the surface low over the Yellow Sea is reduced toward the analysis, but the intensity of the surface high over southern Japan is overestimated in the KA experiments in comparison with those of the AL scheme. According to Table 1, the RMSE and PC become better for both schemes in the order of T126, T214, and T62 at 48 h, whereas the performance is improved as the resolution increases at 72 h. This mixed-resolution dependency of the results at 48 h can be attributed to the absence of data assimilation at the model initial time. Figure 3 compares the time series of the intensity of the surface low during a 36–72-h forecast period. The improvement in the intensity is robust at almost all forecast times, regardless of the horizontal resolution of the model. Without the inclusion of lower-level drag (i.e., as in the AL experiments), the deepening of the surface low is excessive.

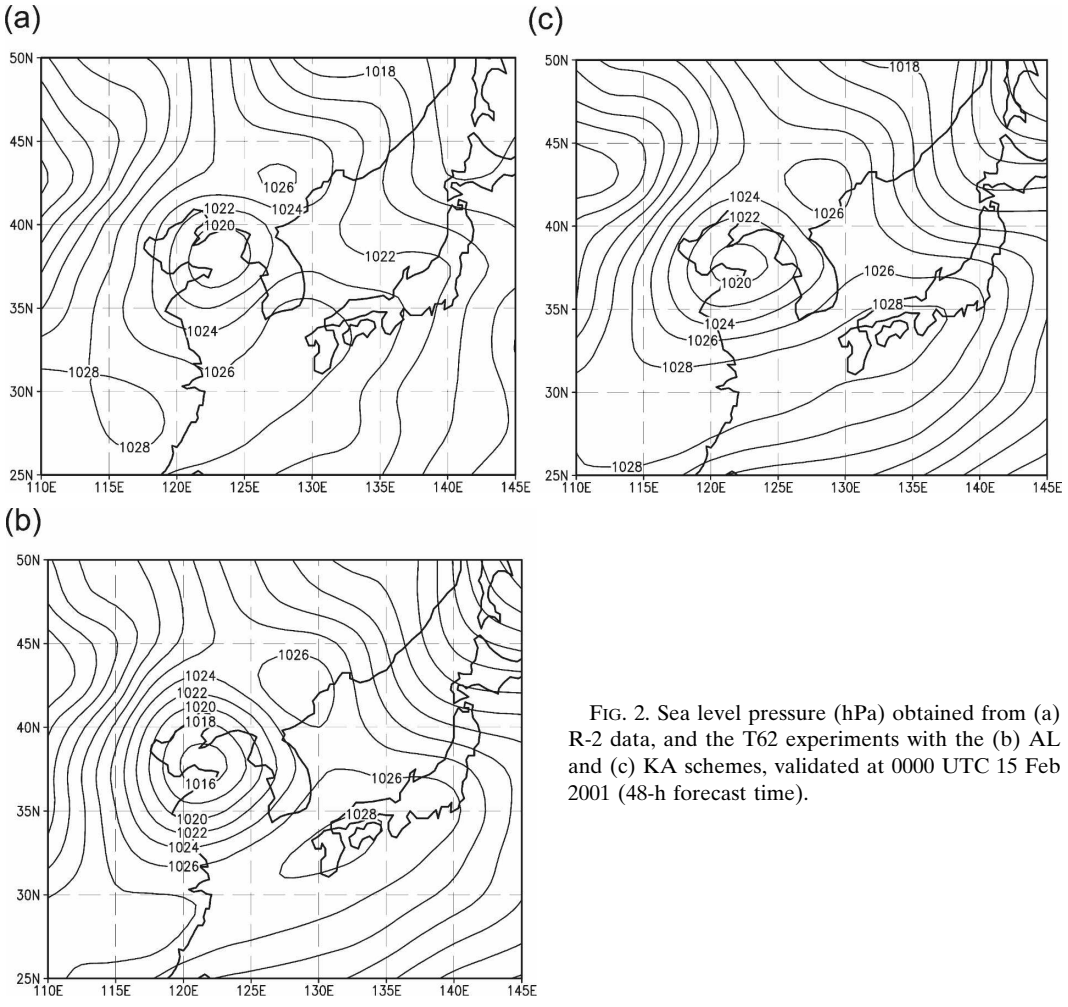

FIG. 2. Sea level pressure (hPa) obtained from (a) R-2 data, and the T62 experiments with the (b) AL and (c) KA schemes, validated at 0000 UTC 15 Feb 2001 (48-h forecast time).

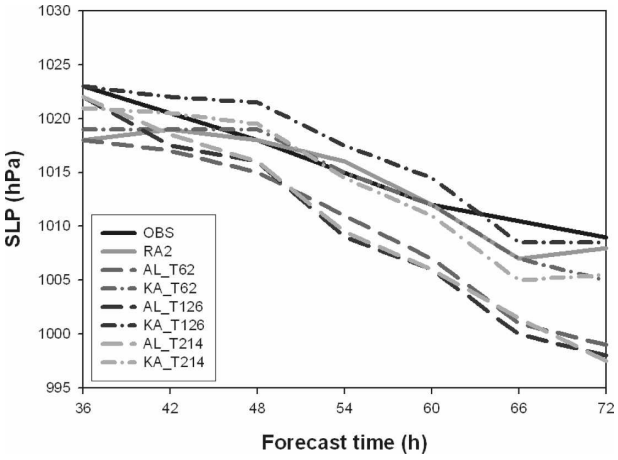

FIG. 3. Time series of the intensity of the surface low during the 36–72-h forecast period.

c. Medium-range forecasts

As an effort to statistically verify the AL and KA experiments, Fig. 4 shows the hemispheric forecast skill scores for the sea level pressure RMSE and 500-hPa geopotential height anomaly correlation (AC) in terms of December 2006 averages of 10-day forecasts. For the verification of medium-range forecasts, AC is widely used to evaluate large-scale forecast skill (Murphy and Epstein 1989). This score shows the relationship between the observed and predicted deviations from climatology of a certain variable. For the NH (Figs. 4a and 4c), it is clear that the KA scheme improves the prediction of large-scale features. The differences in the RMSE between the two schemes are as large as 0.5 hPa after the 5-day forecast. The improvement of the AC is evident from the 5-day forecast, with the skill increasing in time. For the SH (Figs. 4b and 4d), the RSME with the KA scheme is slightly worse than that with the AL scheme. An investigation of the time series of the 500-hPa geopotential height AC and sea level pressure RSME values for individual cases during the month (not shown) verified that the scores in Fig. 4 are statistically significant. The evaluation of other measures of forecast skill in the large-scale fields (not shown) also confirmed that the overall performance of the KA scheme is consistently better in the NH, whereas the skill is slightly worse in the SH. Over the tropics (20°S–20°N; not shown), the difference in the statistical skill between the two runs is small.

It is important to note that the extratropical cyclone shown here is a typical midlatitude cyclogenesis in East Asia in wintertime where the cyclone originating at the eastern flank of the Tibetan Plateau travels northeastward from China to northern Japan across the Korean Peninsula. Moreover, an excessively fast passing of a winter cyclone over the Rockies was alleviated by the inclusion of the enhanced lower drag in the GWDO scheme, as earlier documented by Alpert et al. (1996). Therefore, the overall improvement in the statistical skill scores for the large-scale fields shown in Fig. 4 is considered systematic.

d. Seasonal simulations

Figure 5 compares the seasonal simulations performed with different GWDO parameterizations, which are averages for 3 yr over the 15-member ensembles. The significant changes that occur in the atmospheric structure due to different GWDOs are quite similar for each year, except for those in the location or intensity of the response of the revised GWDO scheme due to the differences in SST forcing. The biases shown by the shading in the figure are 3-yr averages of the deviations of the simulations from the corresponding reanalysis in each year. It was also confirmed that the areas of the difference fields (shading) are statistically significant with a level of significance greater than 95% (not shown).

It can be seen that both the AL and KA schemes generally reproduce the seasonal mean states of the zonal-mean zonal wind and temperature (Figs. 5a,b and 5d,e, respectively). The midlatitude jets in both hemispheres and the temperature distributions depict a typical climatological distribution of the winds and temperature. A distinctive difference between the two schemes appears in the midlatitude jets in both hemispheres. The intensity of the polar night jet is stronger in the KA run than in the AL run, which is due to the overall weaker upper-level wave breaking in the KA scheme (see Fig. 1). The smaller drag in the KA run improves the stratospheric jet intensity in the NH, which was too weak in the AL run by about 20 m s^{-1}; yet the intensity of the SH jet is slightly worse in the KA run by about 5 m s^{-1}. The cold bias, associated with the temperature bias via the thermal wind relation, is generally reduced in the KA scheme in the stratosphere except for a high-latitude region in the NH (cf. Figs. 5e and 5d).

There is little difference in the lower-tropospheric zonal wind between the two experiments whereas the surface pressure has much larger differences. This is because the pressure change near the surface occurs not only because of GWDO directly decelerating the wind in that region, but also because of the secondary meridional circulation induced by the upper-level GWDO acting remotely on the surface, as earlier shown by Palmer et al. (1986). [Kim et al. (2003) revisit this issue with an illustration; see their Fig. 5.] Overall improvements are observed with the KA scheme over the AL

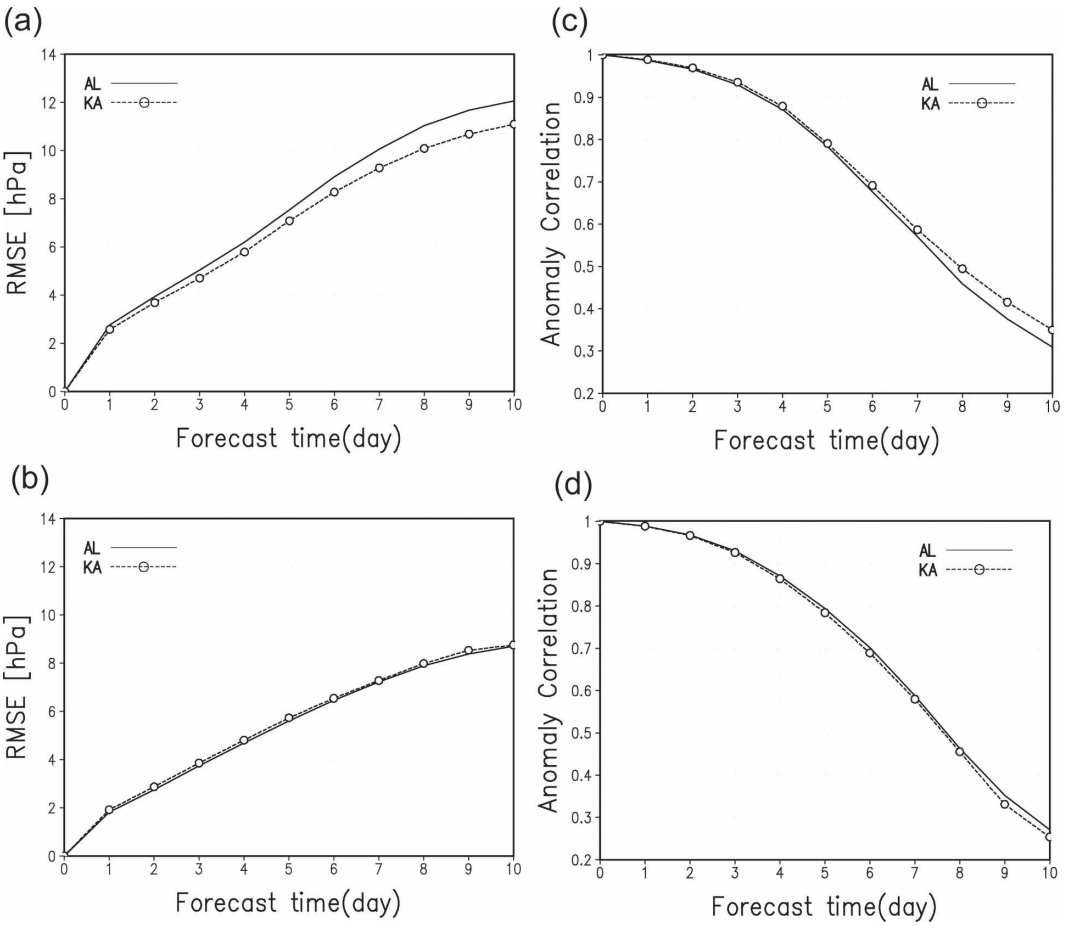

FIG. 4. Monthly mean verification scores of the 10-day forecasts for December 2006 in terms of the sea level pressure RMSE in the (a) Northern and (b) Southern Hemispheres, and (c), (d) the corresponding 500-hPa anomaly correlation coefficients.

scheme in the horizontal distribution of the large-scale climatology, such as the sea level pressure, and the geopotential heights in the troposphere and stratosphere (not shown).

As noted above, the simulation with the KA scheme involves an improvement of the polar night jet in the stratosphere, but also a significant degradation of the subtropical jet (cf. Figs. 5a and 5b). This deficiency is largely corrected when a different value for the critical Richardson number ($Ri_c = 0.75$), which controls the wave-breaking criteria, is used instead of the default value of 0.25 (Fig. 5c). Larger direct momentum deposition between the polar night and subtropical jets with $Ri_c = 0.75$ helps break the jets more realistically. Also improved is the corresponding temperature bias over the tropical stratosphere (Fig. 5f), which was present both in the AL simulation (Fig. 5d) and the original KA simulation (Fig. 5e).

A common problem in all of the simulations appears as too strong easterly winds in the tropical upper troposphere, which may be due to a deficiency associated with the convective precipitation physics and, thus, cannot be properly fixed by GWDO. Another problem is the overestimation of the stratospheric winds in the SH, which is associated with the SH systematic cold bias. This cold bias is distinct in the whole stratosphere, with its vertical range extending in high latitudes and its magnitude increasing upward over the tropics. This bias may be related to the weak absorption of gases in the radiation processes. It has also been reported that this SH bias can be alleviated by the parameterization of GWD due to convective systems (e.g., Chun et al. 2001).

4. Concluding remarks

This study has examined the impacts of enhanced lower-tropospheric GWD induced by subgrid-scale orography on the short- and medium-range forecasts and seasonal simulations in the NCEP GSM. The performance of the GWDO scheme developed by Kim and Arakawa (1995; KA) was evaluated against a tradi-

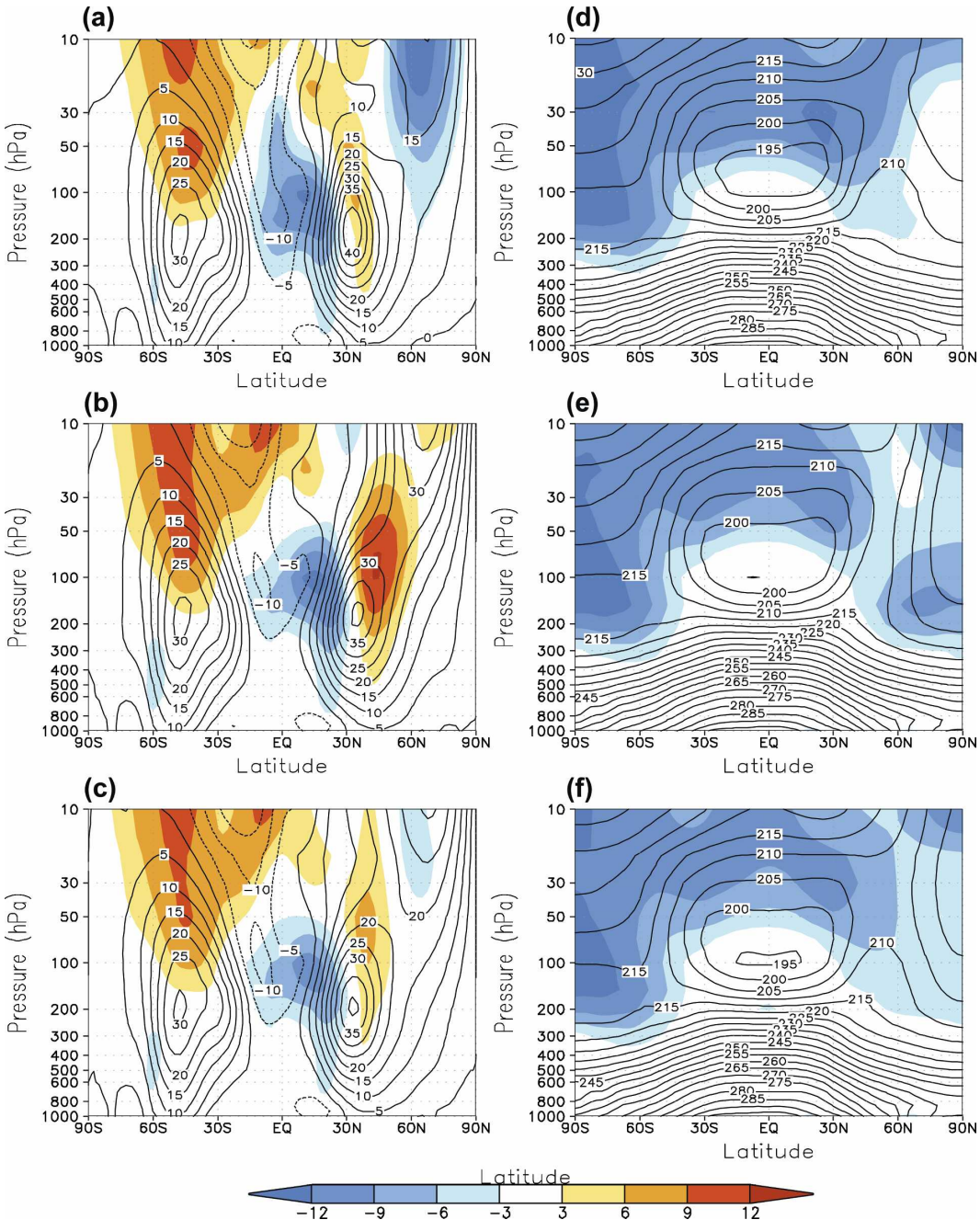

FIG. 5. Three-winter ensemble averages of the (left) zonal wind speed and (right) temperature from the (a), (d) AL and (b), (e) KA schemes (contours) and the biases from the reanalysis (shaded). (c), (f) As in (b), (e) but with $Ri_c = 0.75$.

tional upper-level drag scheme discussed in Alpert et al. (1988) and AL. This study revealed that the KA scheme improved the movement and intensity of an extratropical cyclone and a continental high that was accompanied by heavy snowfall over Korea on 14–15 February 2001. Overall improvements in the medium-range forecast skill for large-scale fields during the period of December 2006 are achieved in the Northern Hemisphere. The simulated 15-member ensemble climatology for three boreal winters (1996/97, 1997/98, and 1999/2000) is generally improved when the KA scheme is employed. The impact of the lower-level drag during the boreal summer was not significant (not shown). For a more rigorous evaluation of the new

scheme, a larger number of multiyear experiments are needed to take into account climatological biases as well as planetary-scale wave effects, as was done in Kim (1996).

Although not reported upon in this study, it was found that the success of the KA scheme was closely linked to the choice of the reference level, where the GWDO parameterization begins at low levels, and the treatment of stable PBL in the model. The reference level in this study is determined as the maximum value of the PBL height (KA) and the doubled value of the standard deviation of the subgrid-scale orography following Kim and Doyle (2005). The treatment of the stable PBL was also found to be a critical component. Without the addition of the stable PBL in the Yonsei University PBL (YSUPBL) scheme, which was used in this study, the drag at the reference level was too small, resulting in a too small amount of wave breaking in the upper levels. These deficiencies were also observed when the Hong and Pan (1996) PBL scheme, which was operational at NCEP in 2000, was employed.

The conclusion of this study is that the enhanced lower-level drag induced by the subgrid-scale orography is a key ingredient that should be parameterized in an atmospheric model for numerical weather forecasts as well as seasonal prediction. Another potentially critical issue in GWD parameterization is the drag induced by convective systems and its interaction with GWDO. Preliminary results showed that the performance of the model in both medium-range forecasts and seasonal simulations is improved when both drag components are included. These results will be reported upon elsewhere in the near future.

Acknowledgments. This work was funded by the Korea Meteorological Administration Research and Development Program under Grant CATER_2007_4406. This work was supported by the Brain Korea 21 Project in 2007. YJK was supported by the Office of Naval Research under ONR Program Element 0601153N. The first and last authors appreciate Jordan Alpert's early aid in implementing and testing the KA scheme and in providing updates on drag parameterization work for NCEP models. The authors would like to acknowledge the anonymous reviewers' thorough and valuable comments that significantly improved the manuscript.

REFERENCES

Alpert, J. C., 2004: Subgrid-scale mountain blocking at NCEP. Preprints, *16th Conf. on Numerical Weather Prediction,* Seattle, WA, Amer. Meteor. Soc., P2.4. [Available online at http://ams.confex.com/ams/pdfpapers/71011.pdf.]

——, M. Kanamitsu, P. M. Caplan, J. G. Sela, G. H. White, and E. Kalnay, 1988: Mountain induced gravity wave drag parameterization in the NMC medium-range forecast model. *Preprints, Eighth Conf. on Numerical Weather Prediction,* Baltimore, MD, Amer. Meteor. Soc., 726–733.

——, S.-Y. Hong, and Y.-J. Kim, 1996: Sensitivity of cyclogenesis to lower tropospheric enhancement of gravity wave drag using the environmental modeling center medium range model. Preprints, *11th Conf. on Numerical Weather Prediction,* Norfolk, VA, Amer. Meteor. Soc., 322–323.

Chun, H.-Y., M.-D. Song, J.-W. Kim, and J.-J. Baik, 2001: Effects of gravity wave drag induced by cumulus convection on the atmospheric general circulation. *J. Atmos. Sci.,* **58,** 302–319.

Hong, S.-Y., 1999: New global orography data sets. NCEP Office Note 424, Camp Springs, MD, 21 pp.

——, and H.-L. Pan, 1996: Nonlocal boundary layer vertical diffusion in a medium-range forecast model. *Mon. Wea. Rev.,* **124,** 2322–2339.

——, Y. Noh, and J. Dudhia, 2006: A new vertical diffusion package with an explicit treatment of entrainment processes. *Mon. Wea. Rev.,* **134,** 2318–2341.

Kanamitsu, M., and Coauthors, 2002a: NCEP dynamical seasonal forecast system 2000. *Bull. Amer. Meteor. Soc.,* **83,** 1019–1037.

——, W. Ebisuzaki, J. Woollen, S.-K. Yang, J. J. Hnilo, M. Fiorino, and G. L. Potter, 2002b: NCEP–DOE AMIP-II Reanalysis (R-2). *Bull. Amer. Meteor. Soc.,* **83,** 1631–1643.

Kim, Y.-J., 1996: Representation of subgrid-scale orographic effects in a general circulation model. Part I: Impact on the dynamics of simulated January climate. *J. Climate,* **9,** 2698–2717.

——, and A. Arakawa, 1995: Improvement of orographic gravity wave parameterization using a mesoscale gravity wave model. *J. Atmos. Sci.,* **52,** 1875–1902.

——, and J. D. Doyle, 2005: Extension of an orographic-drag parameterization scheme to incorporate orographic anisotropy and flow blocking. *Quart. J. Roy. Meteor. Soc.,* **131,** 1893–1921.

——, S. D. Eckermann, and H.-Y. Chun, 2003: An overview of the past, present, and future of gravity-wave drag parameterization of numerical climate and weather prediction models. *Atmos.–Ocean,* **41,** 65–98.

Lindzen, R. S., 1981: Turbulence and stress owing to gravity wave and tidal breakdown. *J. Geophys. Res.,* **86,** 9707–9714.

Lott, F., and M. J. Miller, 1997: A new subgrid-scale orographic parameterization: Its formulation and testing. *Quart. J. Roy. Meteor. Soc.,* **123,** 101–127.

Murphy, A. H., and E. S. Epstein, 1989: Skill scores and correlation coefficients in model verification. *Mon. Wea. Rev.,* **117,** 572–582.

Palmer, T. N., G. J. Shutts, and R. Swinbank, 1986: Alleviation of a systematic westerly bias in circulation and numerical weather prediction models through an orographic gravity-wave drag parameterization. *Quart. J. Roy. Meteor. Soc.,* **112,** 1001–1039.

Parrish, D. F., and J. C. Derber, 1992: The National Meteorological Center's Spectral Statistical-Interpolation Analysis System. *Mon. Wea. Rev.,* **120,** 1747–1763.

Reynolds, R. W., and T. M. Smith, 1994: Improved global sea surface temperature analyses using optimum interpolation. *J. Climate,* **7,** 929–948.

Webster, S., A. R. Brown, D. R. Cameron, and C. P. Jones, 2003: Improvements to the representation of orography in the Met Office Unified Model. *Quart. J. Roy. Meteor. Soc.,* **129,** 1989–2010.